Supporting Information for

Rationalizing the carborane *versus* phenyl-driven luminescence in related dicarboxylic ligands and their antenna effect for their Eu^{3+} and Tb^{3+} metal-organic frameworks: A combined experimental and computational study

Zhen Li,[a,b] Claudio Roscini,[c] Rosario Núñez,[a] Francesc Teixidor,[a] Clara Viñas,[a] Eliseo Ruiz,[d]* José Giner Planas[a]*

[a] *Institut de Ciència de Materials de Barcelona (ICMAB-CSIC), Campus UAB, 08193 Bellaterra, Spain.*
[b] *Shandong Provincial Key Laboratory of Monocrystalline Silicon Semiconductor Materials and Technology, College of Chemistry and Chemical Engineering, Dezhou University, Dezhou 253023, China.*
[c] *Catalan Institute of Nanoscience and Nanotechnology (ICN2), CSIC, and The Barcelona Institute of Science and Technology (BIST), Campus UAB, Bellaterra, Barcelona 08193, Spain.*
[d] *Departament de Química Inorgànica i Orgànica and Institut de Recerca de Química Teòrica i Computacional, Universitat de Barcelona, Diagonal 645, 08028 Barcelona, Spain.*

*Emails: jginerplanas@icmab.es, eliseo.ruiz@qi.ub.es

Supplementary Figures and Tables

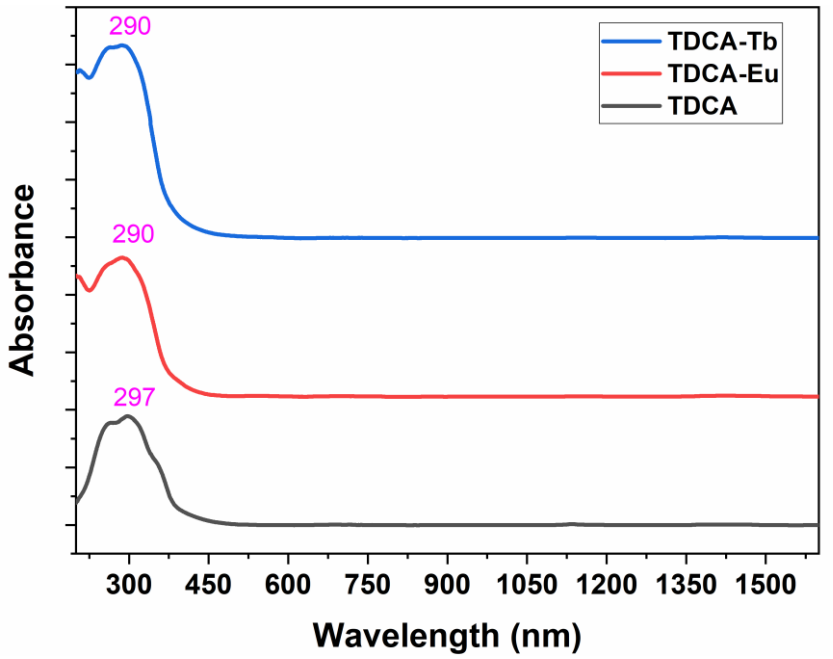

Figure S1. Solid state UV-vis spectra for TDCA and the corresponding Eu and Tb MOFs.

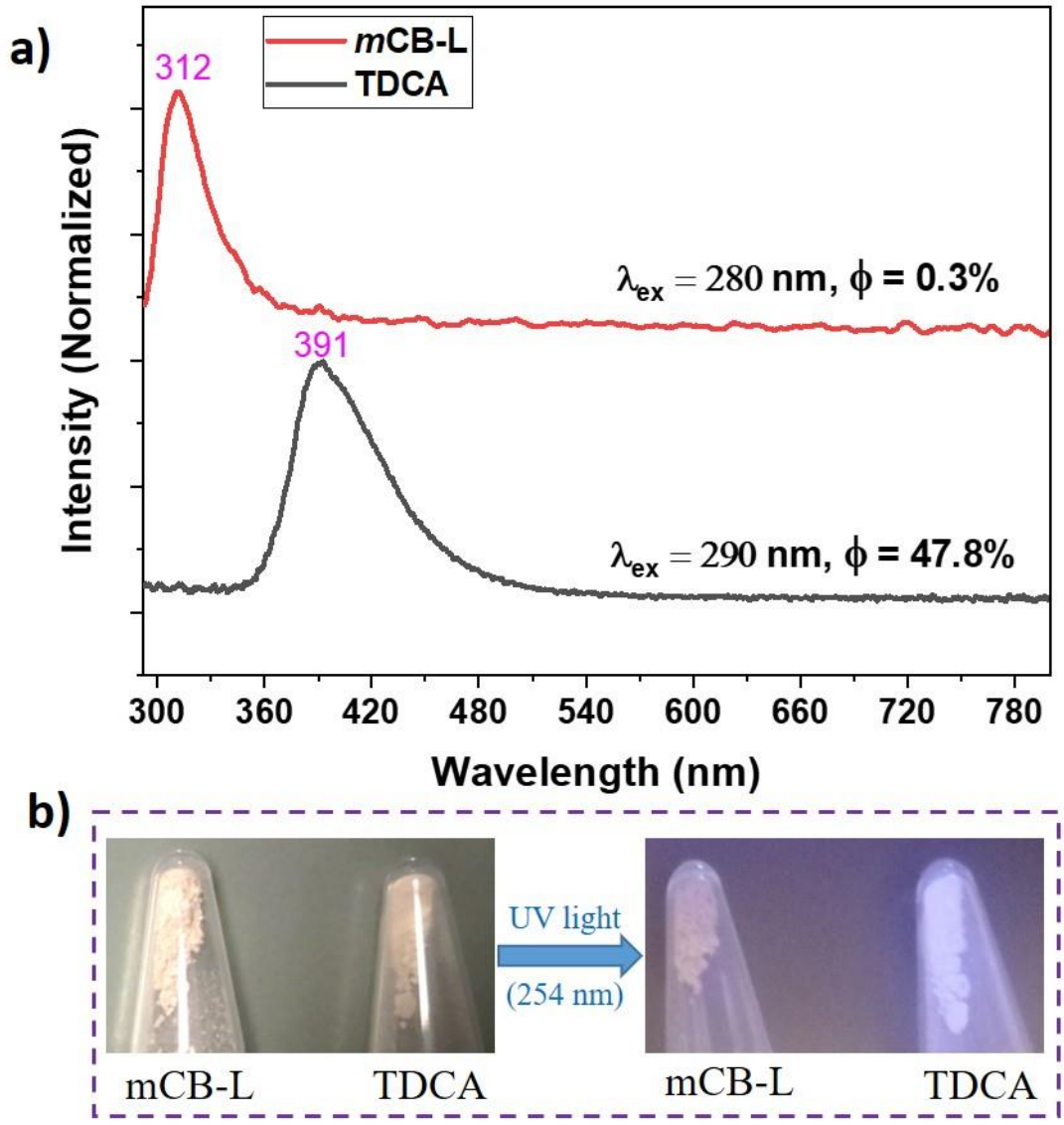

Figure S2. (a) Solid state luminescence spectra for TDCA and *m*CB-L ligand under continuous excitation at the indicated wavelengths; (b) optical images of the corresponding solids under daylight (left), and UV-light (254 nm, right).

Table S1. Calculated singlet-state energy differences (S_0-S_1 and T_1-S_0) for the four studied ligands (in nm and cm^{-1} in parenthesis) using some results at B3LYP TDDFT level from ref. 1 that corresponds to vertical excitations while STEOM-DLPNO-CCSD (see Computational details section) results are vertical (in blue) and adiabatic excitations (in red)). For the two carborane systems, the S_0-S_1 adiabatic excitations are larger than the corresponding vertical ones. The reason for this fact is that the geometries were optimized with a DFT method and the potential surfaces at DFT and coupled cluster are slightly different.

ligand	method	S_0 - S_1	T_1 - S_0
*m*CB-L	B3LYP-TDDFT[1]	260 (38461)	489 (20449)
	STEOM-DLPNO-CCSD	272 (36806)	526 (19006)
		241 (41437)	424 (23593)
*m*CB-L2	STEOM-DLPNO-CCSD	277 (36080)	674 (14818)
		215 (46511)	670 (14932)
TDCA	B3LYP-TDDFT[1]	295 (33898)	607 (16474)
	STEOM-DLPNO-CCSD	280 (35727)	614 (16300)
		294 (34065)	476 (20989)
QDCA	STEOM-DLPNO-CCSD	281 (35583)	685 (14586)
		298 (33565)	512 (19531)

Table S2. Calculated total energies for the four studied ligands (in a.u., and state energy differences in comparison with S_0 in nm and cm^{-1} in parenthesis) using STEOM-DLPNO-CCSD calculations. The optimized geometries for S0, S1, T1 states and the conical intersections (CI) were determined at B3LYP level. The S_0 (T_1 geom) value correspond to the ground state of the optimized structure for the T_1 state.

ligand	state	total energy	energy differences
*m*CB-L	S_0	-1168.960799832	-
	vertical S_1	-1168.793094832	272 (36806)
	minimum S_1	-1168.772000251	241 (41437)
	T_1	-1168.853300111	424 (23593)
	S_0 (T_1 geom)	-1168.939900111	
	CI	-1168.763812552	
*m*CB-L2	S_0	-1630.066756153	-
	vertical S_1	-1629.902363153	277 (36080)
	adiabatic S_1	-1629.854833486	215 (46511)
	T_1	-1629.971344871	670 (14932)
	S_0 (T_1 geom)	-1630.038860871	
TDCA	S_0	-1069.464497967	-
	vertical S_1	-1069.302360967	280 (35727)
	adiabatic S_1	-1069.309286791	294 (34065)
	T_1	-1069.368865172	476 (20989)
	S_0 (T_1 geom)	-1069.443129172	
	CI	-1069.256727594	
QDCA	S0	-1530.586859917	-
	vertical S1	-1530.424733917	281 (35583)
	adiabatic S1	-1530.434024002	298 (33565)
	T1	-1530.497962180	512 (19531)
	S_0 (T_1 geom)	-1530.564419180	

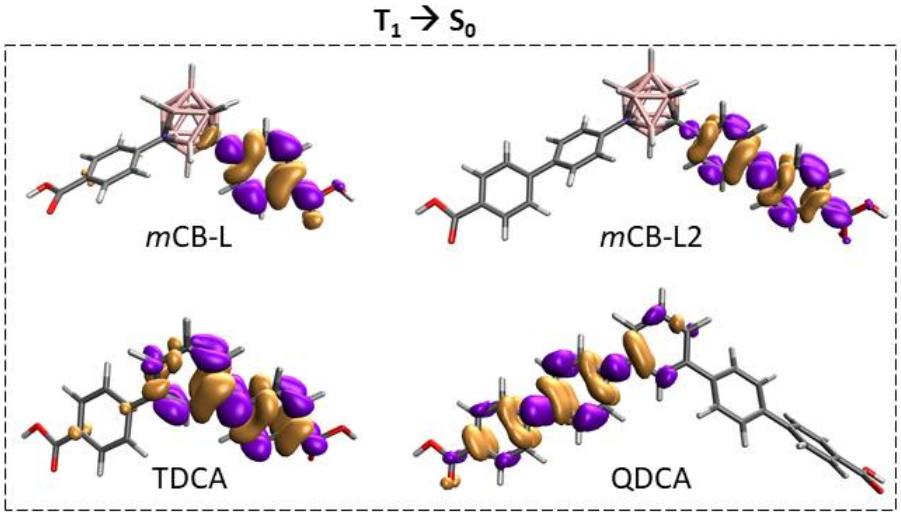

Figure S3. Schematic diagrams for the energy emission from triplet states (T_1 to S_0). Purple (negative values) and pale brown (positive values) lobes represent the electron density differences between the initial and final state calculated at STEOM-DLPNO-CCSD level.

The electron density difference maps corresponding the $T_1 \rightarrow S_0$ de-excitations show that the electron density transferences occur within only one of the sides of the molecule for the four systems. As in the case of the singlet excitations (Fig. 2), the carborane moieties do not show any change in the electron density during the transfer.

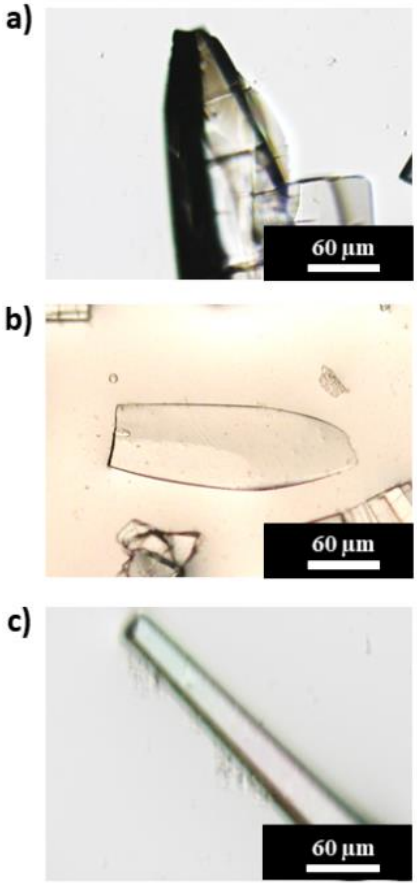

Figure S4. Optical images of the crystals for **TDCA-Ce** (a), **TDCA-Eu** (b) and **TDCA-Tb** (c).

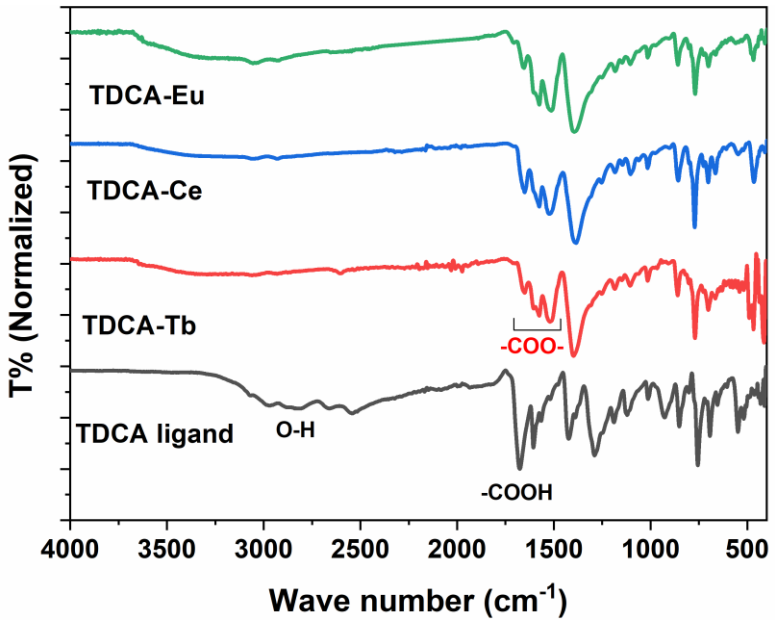

Figure S5. FTIR spectra for TDCA and their Eu, Ce and Tb MOFs.

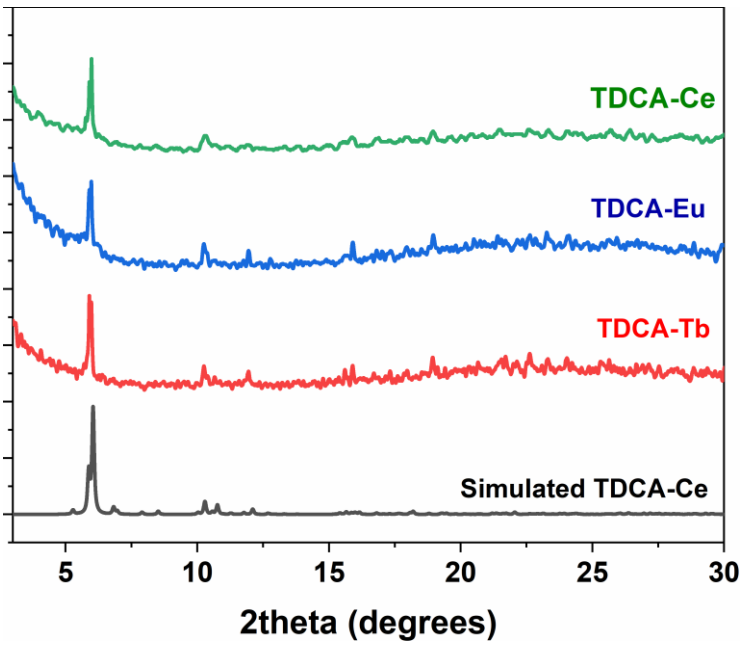

Figure S6. Experimental PXRD patterns of TDCA-Ce, TDCA-Eu and TDCA-Tb, and simulated PXRD pattern of TDCA-Ce.

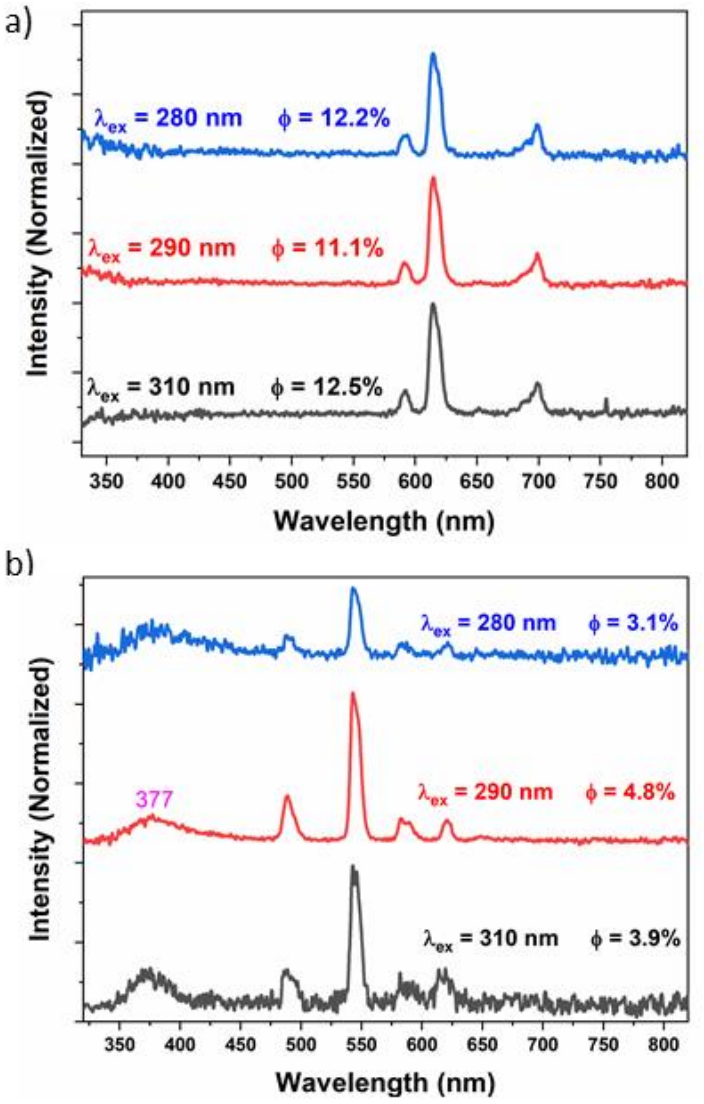

Figure S7. Solid-state emission spectra and quantum yields (QY) of TDCA-**Eu** (a) and TDCA-**Tb** (b) under continuous-wave irradiation at various λ_{ex} (indicated in each spetrum) at room temperature.

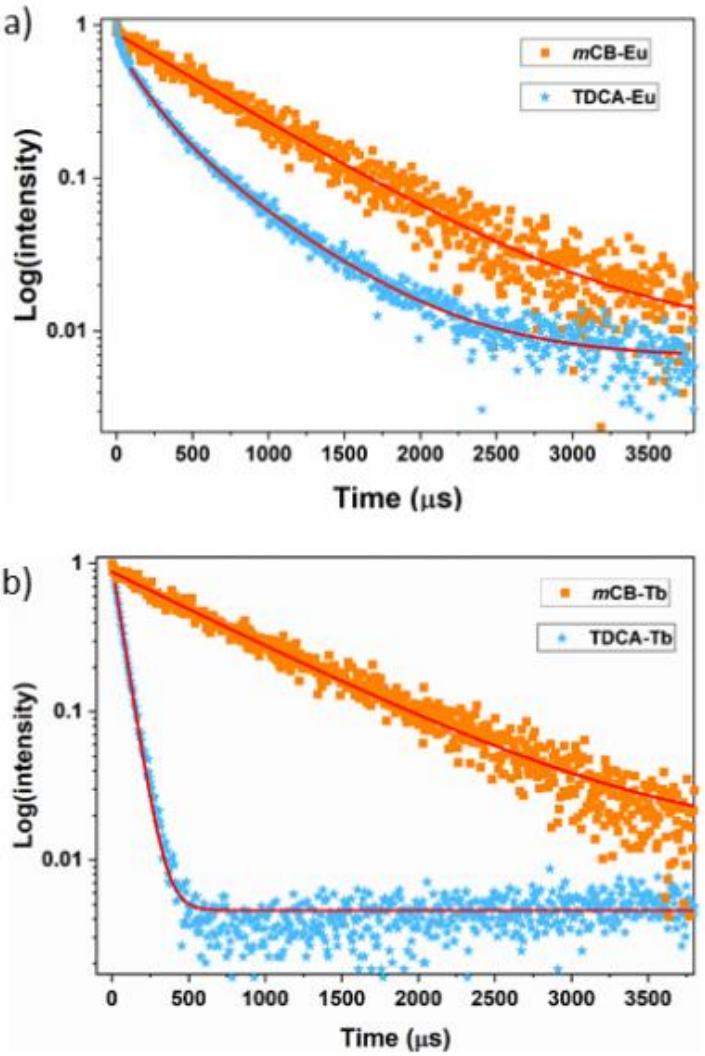

Figure S8. (a) Luminescence decays of Eu (λ_{em} = 614 nm) in the different MOFs (λ_{ex} = 290 nm); (b) Luminescence decays of Tb (λ_{em} = 541 nm) in the different MOFs (λ_{ex} = 290 nm).

References

1 Z. Li, R. Núñez, M. E. Light, E. Ruiz, F. Teixidor, C. Viñas, D. Ruiz-Molina, C. Roscini and J. G. Planas, *Chem. Mater.*, 2022, **34**, 4795–4808.